Progress In Electromagnetics Research C, Vol. 21, 143–153, 2011

EXPERIMENTAL CHARACTERIZATION OF NONLINEAR PULSES IN COUPLED SCHOTTKY TRANSMISSION LINES

K. Narahara

Graduate School of Science and Engineering
Yamagata University
4-3-16 Jonan, Yonezawa, Yamagata 992-8510, Japan

Abstract—We experimentally investigate the properties of nonlinear pulses in coupled transmission lines with regularly spaced Schottky varactors. The c and π modes are different propagation modes that can be developed on a coupled line. Time-domain measurements show that both modes support soliton-like pulses due to the presence of the Schottky varactors; small c-mode pulses are generated by colliding two π-mode pulses traveling in opposite directions. Moreover, we discuss the relationship of the amplitude of the newly generated c-mode pulses with different bias voltages and π-mode-pulse amplitudes.

1. INTRODUCTION

A transmission line periodically loaded with Schottky varactors is called a nonlinear transmission line (NLTL) [1]. NLTLs are used to generate an electrical shock [2], a soliton-like short pulse [3–5] and harmonics waves [6, 7]. For the electrical engineering, a high-power solitons were successfully developed in ceramics [8]. We recently considered the weakly dispersive coupled NLTLs to develop baseband pulses governed by the Korteweg de Vries equation, and proposed a method of doubling the repetition rate of the pulse stream input to the line [9, 10]. The c and π modes are two well-known propagation modes on a linear coupled line [11]. Introducing Schottky varactors preserves the original shape of a pulse traveling along a coupled NLTL because of the balance between dispersion and nonlinearity, irrespective of the propagation mode [9]. We numerically determined that the collision of two π-mode nonlinear pulses leads to the development

Received 23 February 2011, Accepted 27 April 2011, Scheduled 5 May 2011
Corresponding author: Koichi Narahara (narahara@yz.yamagata-u.ac.jp).

of a pair of c-mode pulses (one traveling forward and the other backward) [10]. By utilizing the collision-generated pulses, we can develop a high-repetition-rate pulse train. For that, one end of each line is connected with the transmission lines having the π-mode characteristic impedances, while the other end is connected with the c-mode impedances. Each transmission line is terminated with the corresponding matched resistance. By this arrangement, the multiple reflections of the waves carried by both the c and π modes are suppressed; therefore, the outputs are free from the distortions caused by the reflections. When a π-mode pulse stream is input to the π-impedance end, each pulse collides with the pulses consisting of the pulse stream reflected at the other end. By this collisions and the successive in-phase superposition contribute to the increase in the repetition rate of the pulse stream at the output. When the c-mode pulse travels N times faster than the π-mode one, the repetition rate increases $2N$ times.

To examine the properties of nonlinear pulses in a coupled NLTL, we carried out time-domain measurements of a test circuit. As a result, we successfully observed that nonlinearity compensates for dispersive waveform distortions for both the c- and π-mode pulses, and the collision of two π-mode nonlinear pulses generates the c-mode pulses. Numerical calculations solving the transmission equations of a coupled NLTL accurately simulate the measured results. With the aid of numerical calculations, we examined the dependence of the amplitude of the c-mode pulses on the bias voltage and the amplitude of the π-mode nonlinear pulses.

First, we briefly review the fundamental aspects of a coupled NLTL including the circuit configuration and the single-soliton waveform that characterizes nonlinear c- and π-mode pulses. Definitions are also given for variables that characterize the measured results. To reinforce our previous discussion in [9], we introduce the mutual inductance that becomes influential for monolithically integrated lines. Next, we discuss the measurements with several numerically simulated results.

2. FUNDAMENTAL PROPERTIES OF COUPLED NLTLS

Figure 1 shows the diagram of a unit cell of a coupled NLTL. Two NLTLs, denoted by lines 1 and 2, are coupled via C_m and L_m. For line i ($i = 1, 2$), L_i, R_i, and C_i represent the series inductor, series resistor, and shunt Schottky varactor of the unit cell, respectively. Lines 1 and 2 are biased at V_0 and W_0, respectively. The c and π modes are propagation modes on a linear coupled line [11]. These are the same for

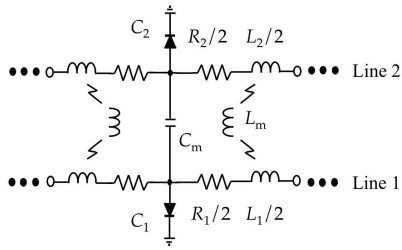

Figure 1. Unit cell of a coupled NLTL.

a coupled NLTL when the voltage amplitude is sufficiently small. Each mode has its own velocity and voltage fraction between the lines (line 2 voltage/line 1 voltage). The quantities u_c, u_π, R_c, and R_π designate, respectively, the velocity of the c mode, the velocity of the π mode, the voltage fraction of the c mode and the voltage fraction of the π mode at long wavelengths. These are explicitly written as

$$u_{c,\pi} = \sqrt{\frac{x_1 + x_2 \pm \sqrt{(x_1 + x_2)^2 - 2x_3}}{x_3}}, \tag{1}$$

$$R_{c,\pi} = \frac{x_1 - x_2 \pm \sqrt{(x_1 + x_2)^2 - 2x_3}}{2c_m l_1}, \tag{2}$$

where the upper (lower) signs are for c (π) mode. For concise notations, we define $x_{1,2,3}$ as

$$x_1 = (C_1(V_0) + C_m)L_1 - C_m L_m, \tag{3}$$

$$x_2 = (C_2(W_0) + C_m)L_2 - C_m L_m, \tag{4}$$

$$x_3 = 2\left[C_1(V_0)C_2(W_0) + (C_1(V_0) + C_2(W_0))C_m\right](L_1 L_2 - L_m^2). \tag{5}$$

In a linear line, the short-wavelength waves travel slower than the long-wavelength waves due to dispersion. This distorts the baseband pulses of short durations. In a coupled NLTL, nonlinearity introduced by Schottky varactors can compensate for this distortion, irrespective of the propagation mode. We model the capacitance voltage relationship of a Schottky varactor as

$$C(x) = \frac{C_0}{\left(1 - \frac{x}{V_J}\right)^m}, \tag{6}$$

where x is the voltage between the terminals, and C_0, V_J, and m are the zero-bias junction capacitance, junction potential, and grading coefficient, respectively. Note that $x < 0$ for reverse bias.

By applying the reductive perturbation method to the transmission equations of coupled NLTLs, we obtained the Korteweg-de Vries equation that describes the nonlinear pulses on the lines [9]. The dispersion coefficient $p_{c(\pi)}$ and the nonlinearity coefficient $q_{c(\pi)}$ are calculated to be

$$\begin{aligned} p_{c,\pi} &= \mp\frac{\sqrt{2}c_m}{\sqrt{(x_1+x_2)^2-2x_3}}\left[x_1+x_2\mp\sqrt{(x_1+x_2)^2-2x_3}\right]^{-3/2} \\ &\quad\times\left[\frac{c_1(V_0)l_1^2m_1}{V_0-V_{J1}}\frac{x_1-x_2\mp\sqrt{(x_1+x_2)^2-2x_3}}{x_1-x_2\pm\sqrt{(x_1+x_2)^2-2x_3}}\right. \\ &\quad\left.+\frac{c_2(W_0)l_2^2m_2}{W_0-V_{J2}}\frac{x_1-x_2\pm\sqrt{(x_1+x_2)^2-2x_3}}{x_1-x_2\mp\sqrt{(x_1+x_2)^2-2x_3}}\right], \end{aligned} \tag{7}$$

$$q_{c,\pi} = \frac{1}{24}\sqrt{\frac{x_1+x_2\pm\sqrt{(x_1+x_2)^2-2x_3}}{x_3}}, \tag{8}$$

where the upper (lower) signs are for the c (π) mode, and m_i and V_{Ji} are the varactor model parameters for the line i ($i = 1, 2$). Then, a single-soliton solution with an amplitude of A_0 is given by

$$V(x,t) = V_0 - A_0\,\mathrm{sech}^2\left[\sqrt{\frac{pA_0}{12q}}\left[x-\left(u+\frac{pA_0}{3}\right)t\right]\right], \tag{9}$$

$$W(x,t) = W_0 - RA_0\,\mathrm{sech}^2\left[\sqrt{\frac{pA_0}{12q}}\left[x-\left(u+\frac{pA_0}{3}\right)t\right]\right], \tag{10}$$

where (p, q, u, R) is set to $(p_{c(\pi)}, q_{c(\pi)}, u_{c(\pi)}, R_{c(\pi)})$ for the c (π)-mode soliton. Note that A_0 is set positive (negative) for $p > (<)0$.

3. EXPERIMENTS

We used the 112-section coupled NLTL, whose unit section is shown in Fig. 1, with $L_m = 0$. The circuit was built on a standard breadboard by using TOSHIBA 1SV101 diodes as the Schottky varactors. TDK SP0508 inductors of 10.0 and 4.7 μH provided inductances for lines 1 and 2, respectively, and 47 pF TDK FK24C0G1 capacitors provided mutual capacitance. For the model parameters we employed, u_c, u_π, R_c, and R_π are calculated using Eqs. (1) and (2) to be 7.36×10^7 cell/s, 3.25×10^7 cell/s, 1.25, and -0.38, respectively. An Agilent 1134 active probe detected signals along the test line and an Agilent DSO90254A oscilloscope monitored them in the time domain.

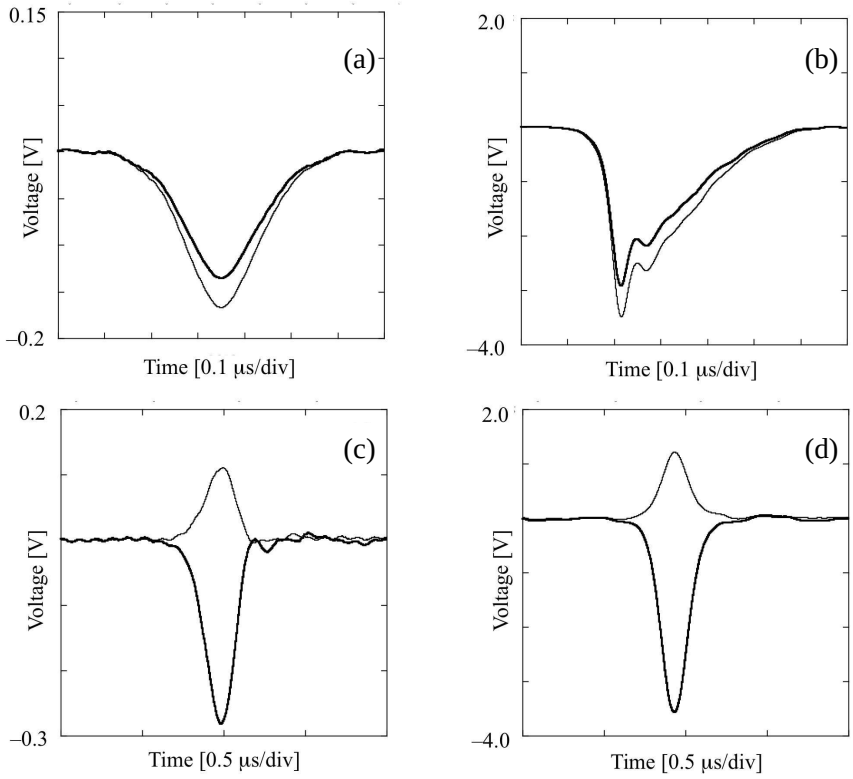

Figure 2. Linear and nonlinear pulses in test coupled NLTL. (a) The c-mode linear pulse, (b) the c-mode nonlinear pulse, (c) the π-mode linear pulse, and (d) the π-mode nonlinear pulse. The thick and thin waveforms correspond to the waveform monitored at the 50th cell on lines 1 and 2, respectively.

For characterization of the c-mode pulses, a two-channel arbitrary waveform generator (NF WF1974) generated two pulses having identical amplitude and parity and fed them to the first cells of lines 1 and 2, whereas the 121st cells of both the lines were terminated with DC sources. Both bias voltages, V_0 and W_0, were set to -3.0 V. Figs. 2(a) and (b) show the c-mode pulses monitored at the 50th cells on lines 1 and 2 with small and large amplitudes, respectively. The thick and thin curves correspond to the waveforms on lines 1 and 2, respectively. In Fig. 2(a), the linear pulse was weakly distorted by dispersion. R_c well characterizes the amplitude fraction between lines 1 and 2, which is estimated to be 1.23. On the other hand, the pulse

exhibits several peaks developed by the evolving multiple soliton-like pulses. Note that the voltage fraction between lines 1 and 2 is the same as that of the linear counterpart. Figs. 2(c) and (d) show the π-mode pulses monitored at the 50th cells on lines 1 and 2 with small and large amplitudes, respectively. The pulse input to line 2 had the opposite parity and was half as large as that input to line 1. Fig. 2(c) shows that dispersion delayed the high frequency waves more than the low-frequency waves owing to dispersion. Nonlinearity well compensated for this distortion in Fig. 2(d). The voltage fraction between the lines, which is estimated to be -0.40, is well characterized by R_π for both linear and nonlinear cases. Furthermore, the waveform in Fig. 2(d) is well fitted by Eqs. (9) and (10) for $A_0 = 1.0\,\mathrm{V}$.

Figure 3 shows the spatio-temporal waveforms on line 2 that describe the collision of two π-mode nonlinear pulses. Two phase-synchronized NF WF1974 generators provide signals, with the first cells of lines 1 and 2 connected to one generator, the other generator feeds pulses to the 121st cells of lines 1 and 2. The temporal delay between the pulse incidence at the first cells and that at the 121st cells was set to cause a collision at the 70th cells. Fig. 3 shows that small and fast pulses, one traveling forward and the other backward,

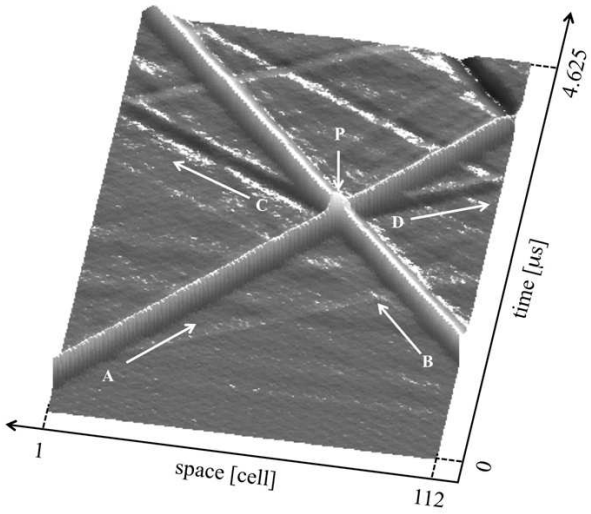

Figure 3. Generation of c-mode pulses by colliding π-mode nonlinear pulses. Trajectories A and B correspond to the two π-mode nonlinear pulses, which collided at point P. Trajectories C and D correspond to the generated c-mode pulses.

originated at the collision point P. The velocity and the voltage fraction of the generated pulses were close to u_c and R_c, respectively; thus, establishing that the collision of two π-mode nonlinear pulses generates the c-mode pulses.

4. DISCUSSION

To investigate the properties of interacting nonlinear pulses, we numerically solve the transmission equations by using a standard finite-difference time-domain method for a coupled NLTL with the Schottky varactors having $C_0 = 64.77\,\text{pF}$, $V_J = 3.561\,\text{V}$, and $m =$

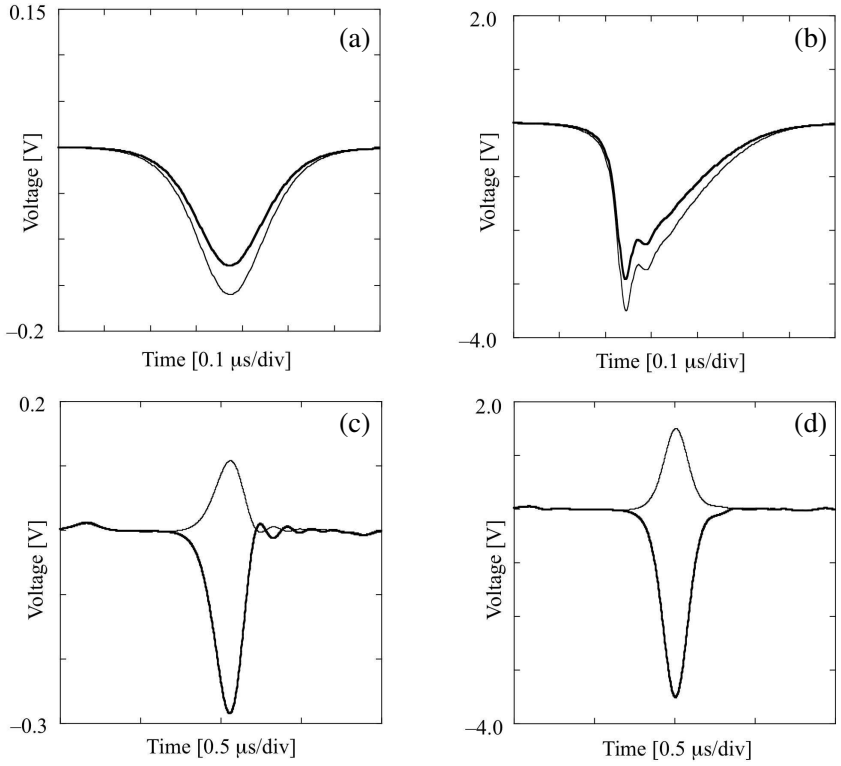

Figure 4. Calculated linear and nonlinear pulses in test coupled NLTL. (a) The c-mode linear pulse, (b) the c-mode nonlinear pulse, (c) the π-mode linear pulse, and (d) the π-mode nonlinear pulse. The thick and thin waveforms correspond to the waveform monitored at the 50th cell on lines 1 and 2, respectively.

1.259 in Eq. (6). First, we examine how the numerical calculations simulate the measured results. Figs. 4(a), (b), (c), and (d) show the calculated waveforms corresponding to the measured ones shown in Figs. 2(a), (b), (c), and (d), respectively. For linear pulses, the similarity between the measured and calculated waveforms is perfect. Even for the nonlinear pulses, the soliton-like properties, such as the development of multiple peaks in Fig. 4(b) and the compensation of dispersive distortion in Fig. 4(d), are correctly simulated. Thus, we concluded that the calculation method accurately predicts the phenomenon in a coupled NLTL.

At present, the amplitude of the c-mode pulses generated by colliding nonlinear π-mode pulses is considerably small. Broadening the range of applications for coupled NLTLs requires design criteria that obtain larger c-mode amplitudes. As a first step, we investigate the dependence of c-mode pulse amplitude on manageable parameters. Figs. 5(a) and (b) show the dependence of c-mode pulse amplitude on the bias voltages applied to lines 1 and 2 and the amplitude of colliding π-mode pulses, respectively. To obtain Fig. 5(a), we varied the bias voltages from -4.0 to -1.0 V in 0.5-V increments, keeping a common bias voltage on lines 1 and 2. Qualitatively, c-mode pulses should increase in amplitude as the bias increases, because the Schottky varactors exhibit stronger nonlinearity for higher bias voltages, and

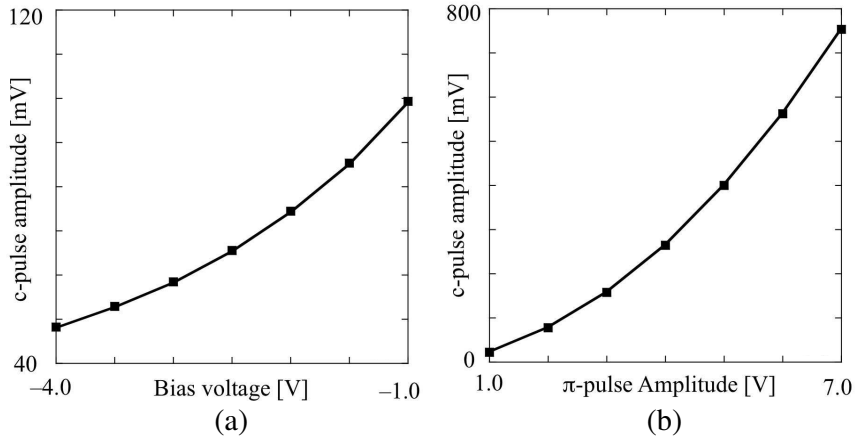

Figure 5. Calculated amplitude of c-mode pulses generated by colliding π-mode nonlinear pulses. The dependence of the c-pulse amplitude on (a) the bias voltages applied to lines 1 and 2 and (b) the amplitude of colliding π-mode nonlinear pulses.

this was verified. Moreover, the c-mode amplitude in Fig. 5(a) is well fitted by $31.3 + 108.3 * e^{0.46*V_0}$ mV. A similar exponential dependence is observed in Fig. 5(b), which is fitted by $-253.7 + 215.6e^{0.22*V_\pi}$ mV. These exponential increases are useful for obtaining large c-mode pulses.

Figure 6 shows the measured dependence of the c-mode pulse amplitude on the bias voltages. Fig. 6(a) shows the waveforms monitored at the 22nd cell, where the c-mode pulses are well separated from the π-mode nonlinear pulses. The thick, thin, and dotted waveforms correspond to the bias voltages of -2.0, -3.0, and -4.0 V, respectively. The pulses designated by F and B show the forward and backward π-mode pulses, respectively. A dashed circle encloses the target c-mode pulses, and the refined waveforms are shown in Fig. 6(b). The amplitude of the c-mode pulse increases as the bias voltage increases. Fig. 6(c) shows the dependence. The c-mode amplitude increases from -4.0 to -2.0 V. These measured results qualitatively validate the possibility of increasing the amplitude of c-mode pulses. Unfortunately, the collision-generated c-mode pulses cannot be fully simulated by our numerical model. The discrepancy between the measured and calculated amplitude dependences are mainly due to the insufficient modeling of the Schottky varactors. For smaller V_J

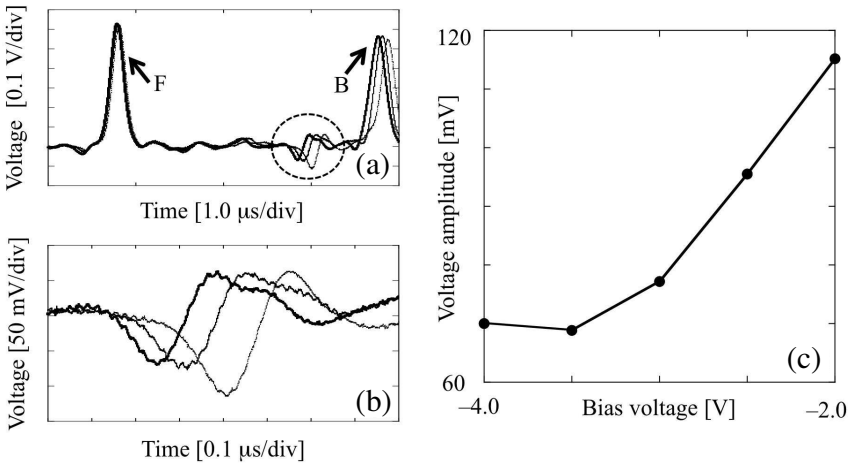

Figure 6. Measured amplitude of c-mode pulses generated by colliding π-mode nonlinear pulses. (a) The waveforms on line 2 monitored at the 22nd cell, (b) the waveforms of c-mode pulses, and (c) the dependence of c-pulse amplitude on the bias voltages applied to lines 1 and 2.

and larger m, the varactor exhibits stronger nonlinearity. As a result, the amplitude of collision-generated pulses increases for such parameter values. The yield of the varactor also influences the amplitude. It is found that the c-mode amplitude decreases as the yield rate increases through numerical calculations. Moreover, the loss elements such as the parasitic resistances in inductors are another factors that determine the c-mode amplitudes. The attenuation of incident π-mode pulses reduces the amplitudes of the collision-generated c-mode pulses, which too become attenuated. In general, the loss elements attenuate the waves carried by the π mode more than the c-mode waves. Moreover, the rate of attenuation depends on the bias voltage. Numerical evaluation suggests that the amplitude reduction of collision-generated pulses becomes more eminent for larger bias voltages.

5. CONCLUSION

Every mode can support soliton-like pulses in coupled NLTLs, and the collision of π-mode nonlinear pulses generates c-mode pulses. For higher bias voltages and larger π-mode amplitudes, the c-mode pulse amplitude increases. These unique properties give coupled NLTLs great potential for managing short electrical pulses.

REFERENCES

1. Hirota, R. and K. Suzuki, "Studies on lattice solitons by using electrical networks," *J. Phys. Soc. Jpn.*, Vol. 28, 1366–1367, 1970.
2. Rodwell, M. J. W., S. T. Allen, R. Y. Yu, M. G. Case, U. Bhattacharya, M. Reddy, E. Carman, M. Kamegawa, Y. Konishi, J. Pusl, and R. Pullela, "Active and nonlinear wave propagation devices in ultrafast electronics and optoelectronics," *Proc. IEEE*, Vol. 82, 1037–1059, 1994.
3. Kintis, M., X. Lan, and F. Fong, "An MMIC pulse generator using dual nonlinear transmission lines," *IEEE Microwave Wireless Compo. Lett.*, Vol. 17, 454–456, 2007.
4. Yildirim, O. O., D. S. Ricketts, and D. Ham, "Reflection soliton oscillator," *IEEE Trans. Microwave Theory Tech.*, Vol. 57, 2344–2353, 2009.
5. Ryjenkova, I. V., V. K. Mezentsev, S. L. Musher, S. K. Turitsyn, R. Hülsewede, and D. Jäger, "Millimeter wave generation on nonlinear transmission lines," *Ann. Telecommun.*, Vol. 52, 134–139, 1997.

6. Jäger, D., "Characteristics of traveling-waves along nonlinear transmission lines for monolithic integrated circuits: A review," *Int. J. Electron.*, Vol. 58, 649–669, 1985.
7. Wedding, B. and D. Jäger, "Phase-matched second harmonic generation and parametric mixing on nonlinear transmission lines," *Electron. Lett.*, Vol. 17, 76–77, 1981.
8. Ikezi, H., J. S. Degrassie, and J. Drake, "Soliton generation at 10 MW level in the very high frequency band," *Appl. Phys. Lett.*, Vol. 58, 986–987, 1991.
9. Narahara, K., "Coupled nonlinear transmission lines for doubling repetition rate of incident pulse streams," *Progress In Electromagnetics Research Letters*, Vol. 16, 69–78, 2010.
10. Narahara, K., "Interaction of nonlinear pulses developed in coupled transmission lines regularly spaced Schottky varactors," *Progress In Electromagnetics Research Letters*, Vol. 17, 85–93, 2010.
11. Gupta, K. C., R. Garg, and I. J. Bahl, *Microstrip Lines and Slotlines*, Artech, 1979.